

A chaincode based scheme for fingerprint feature extraction

Zhixin Shi *, Venu Govindaraju

Center of Excellence for Document Analysis and Recognition (CEDAR), State University of New York at Buffalo, Amherst 14228, USA

Received 17 February 2004; received in revised form 18 August 2005

Available online 20 October 2005

Communicated by T.K. Ho

Abstract

A feature extraction method using the chaincode representation of fingerprint ridge contours is presented. The representation allows efficient image quality enhancement and detection of fine minutiae feature points. The direction field is estimated from a set of selected chaincodes. The original gray-scale image is enhanced using a dynamic filtering scheme that takes advantage of the estimated direction flow of the contours. Minutiae are generated using ridge contour following.

© 2005 Elsevier B.V. All rights reserved.

Keywords: Fingerprint; Minutiae; Features extraction; Biometrics; Chaincode

1. Introduction

Automatic Fingerprint Identification System (AFIS) is an important biometric technology that is widely used. A fingerprint is the pattern of ridges and valleys on the surface of a fingertip. The uniqueness of a fingerprint is determined by the local ridge characteristics and their relationships (Lee and Gaensslen, 1991; Moenssens, 1971). The two most prominent characteristics are the ridge ending and the ridge bifurcation, called minutiae. Most automatic systems for fingerprint comparison are based on minutiae matching (Jain et al., 1997; Ratha et al., 1996). A good quality fingerprint typically contains about 40 to 100 minutiae. A critical step in fingerprint matching is to automatically and reliably extract minutiae.

Fingerprint images can be obtained from ink impressions or by direct live scanning by sensors (Xia and O’Gorman, 2002) such as ultrasound (Schneider and Glenn, 1996). Due to imperfections of the image acquisition processes, minutiae extraction methods are prone to missing some real minutiae while picking spurious ones (Jain

et al., 1997; Ratha et al., 1996). Errors could also occur in the location coordinates of the true minutiae and their relative orientation in the image.

Minutiae can be extracted from binary fingerprint images (Ratha et al., 1995, 1996; Jain et al., 1997) or directly from gray-scale images (Maio and Maltoni, 1997). Most algorithms described in the literature extract minutiae from a thinned skeleton image. Thinning is a lossy and computationally expensive operation and the accuracy of the output skeletal representation varies. In this paper we introduce the use of chaincode representation (Wilf, 1981) as an efficient alternative. Given a binary image, it is scanned from top to bottom and right to left, and transitions from white (background) to black (foreground) are detected. The contour is then traced counterclockwise (clockwise for interior contours) and expressed as an array of elements (Fig. 1). Each contour element represents a pixel on the contour, and contains fields for the x , y coordinates of the pixel, the slope or direction of the contour into the pixel, and auxiliary information such as curvature.

We present two chaincode based algorithms for fingerprint image enhancement (Section 2) and minutiae feature extraction (Section 3). Experimental results are presented in Section 4.

* Corresponding author. Fax: +1 716 645 6176.
E-mail address: zshi@cedar.buffalo.edu (Z. Shi).

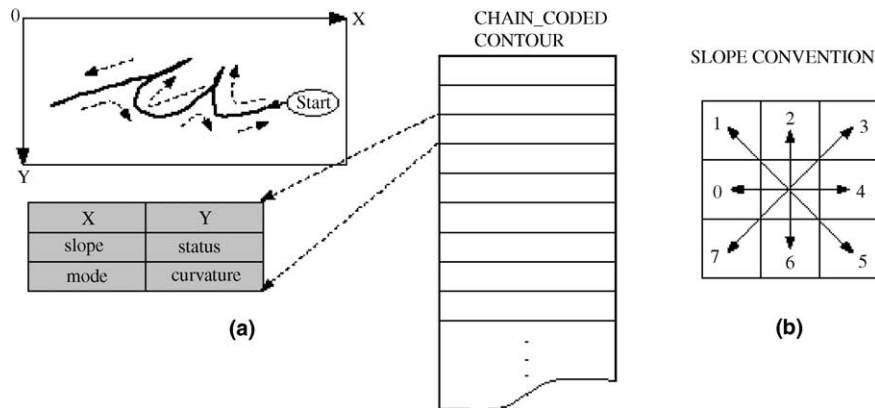


Fig. 1. Chain code contour representation: (a) contour element, (b) slope convention. Data field in the array contains positional and slope information of each component of the traced contour. Properties stored in the information fields are: coordinates of bounding box of a contour, number of components in the corresponding data fields, area of the closed contour, and a flag which indicates whether the contour is interior or exterior.

2. Fingerprint image enhancement

Binarization techniques often render images unsuitable for extraction of fine and subtle features such as minutiae points. The objective of enhancement is to: (i) improve the clarity of ridge structures of fingerprint images, (ii) maintain their integrity, (iii) avoid introduction of spurious structures, and (iv) retain the connectivity of the ridges while maintaining separation between ridges.

There are two types of fingerprint image enhancement methods described in the literature; those that work on binary images and those that work on gray-scale images (Maio and Maltoni, 1997; O’Gorman and Nickerson, 1989; Sherlock et al., 1994). The methods using binary images require a specially designed binarization algorithm to ensure that the connectivity information lost during binarization can be at least partially restored. The methods directly using gray-scale images start with a direction field (that captures the local orientation information of the ridge contours) followed by the application of a bank of filters (Hong et al., 1998). The direction field is computed by the gradient method which is inefficient and unstable in noisy images.

The method presented in this paper combines both the binary and the gray-scale image enhancement methods. We first use a locally adaptive algorithm to obtain a binary fingerprint image of sufficient quality. The local direction field is estimated using a fast chaincode-base algorithm and a 15×15 mask. Larger masks retain the orientation while compromising the integrity of the ridges. This is followed by applying an elliptically shaped filter (Greenberg et al., 2002) with its major axis aligned parallel to the local ridge direction. This increases the connectivity along the ridge direction.

Experiments on DB4 NIST Fingerprint Image Groups show that a single global threshold based binarization can not handle noise from non-uniform ink density, non-printed areas, and other stains. In order to smooth edges of the ridge contours, a 3×3 mask is applied to the gray-scale image as a quick equalization process before applying the locally adaptive thresholding described (Giuliano et al.,

1977). Contrast enhancement by statistics based normalization (O’Gorman and Nickerson, 1989; Greenberg et al., 2002; Simon-Zorita et al., 2001) often cause interference between sweat pores and ridge edges. For minutiae extraction the sweat pores should be eliminated. Fig. 2 shows examples of fingerprint images from FVC2004: the Third International Fingerprint Verification Competition (Maio et al., 2004), and the binary images obtained by our method. We have tested on images from FVC2004 (320 images) and NIST database (30 images). Many ridges are broken in the binary image and therefore is not good for minutiae extraction. However, the quality is sufficient for generating local ridge orientations for image enhancement.

2.1. Chaincode processing

Chaincode representation of object contours is extensively used in document analysis (Wilf, 1981; Madhvanath et al., 1997; Feldbach and Tonnes, 2001; Shi and Govindaraju, 1997). Unlike thinned skeletons, the pixel image can be fully recovered from the chaincode of its contour.

Tracing the chaincode contour, provides local ridge directions at each boundary pixel. We divide the image into 15×15 pixel blocks and use the ridge directions to estimate the orientation of each block. The algorithm is as follows.

- Use the width of ridges as a guide to estimate the threshold under which components are likely to be noise.
- End points are detected (Section 3) and not made part of the computation of the direction flow field as directions around end points tend to be ambiguous.
- The ridge orientation is computed using the eight chaincode directions of contour points in each block. A voting algorithm is used to select the dominant direction as the local orientation.

The threshold used for filtering noise can be dynamically estimated from the average size of the ridge width. The minimum number of contour points in a block to

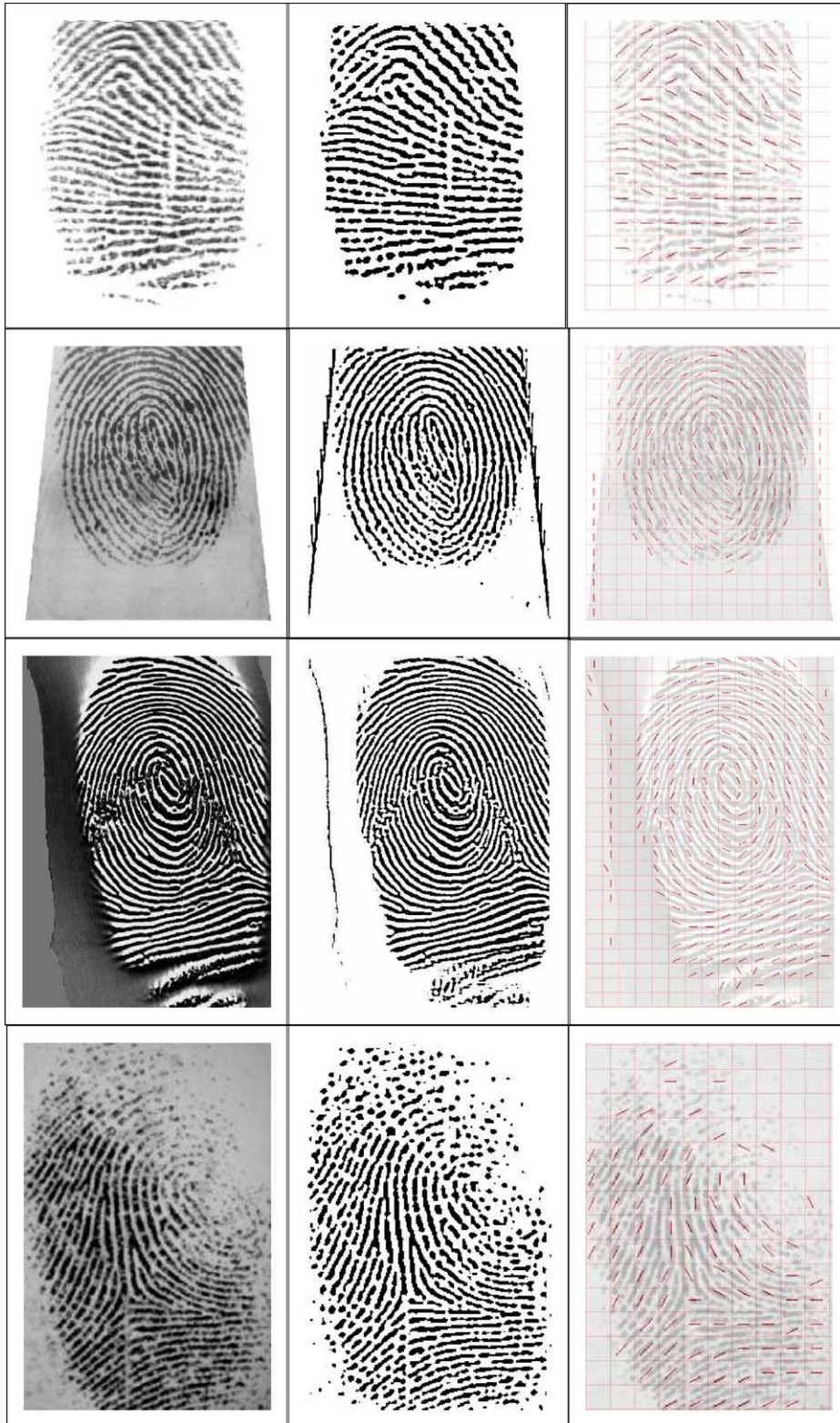


Fig. 2. Local-adaptive binarization and direction field generation using chaincode representation. Example images on the first column are from FVC2004: the Third International Fingerprint Verification Competition, the images from devices with various qualities and resolutions. The second column are the binary images using the Local-adaptive algorithm and the third column are direction field images which demonstrate satisfactory local directions for enhancement.

derive orientation is determined based on the block size and is about 30 in our experiments.

There are many direction field estimation algorithms described in the literature (Hong et al., 1998; Greenberg et al.,

2002; Simon-Zorita et al., 2001). These are designed primarily for extraction of ridge flow and minutiae and not for image enhancement. Donahue and Rokhlin (1993) and Maio and Maltoni (1997) use a gradient operator to extract a directional estimate from each 2×2 pixel neighborhood. The direction field is computed using least-squares minimization of the gradients in the local windows. However, the method becomes computationally expensive if the local windows used are large. Our method of direction field generation using chaincode for image enhancement is more efficient and robust for the following reasons: (i) chaincode generation depends on a pre-binarization algorithm, (ii) the adaptive binarization algorithm and the chaincode generation algorithm are both efficient, and (iii) the orientation field is directly computed by tracing the chaincode over a discrete grid. The objective is to attain the ridge orientation for the entire window rather than at every pixel. Fig. 2 shows the direction fields generated for the FVC2004 fingerprint images and Fig. 3 shows the same for a NIST fingerprint image.

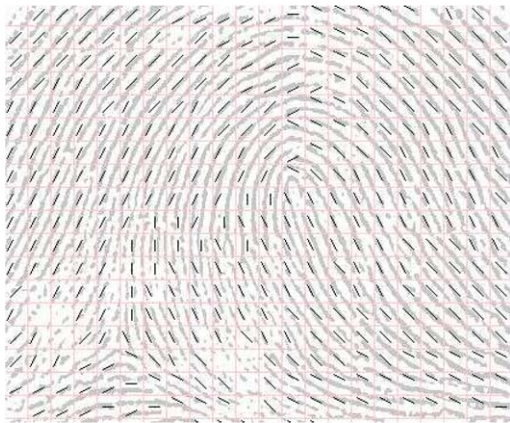


Fig. 3. Direction field image generated using chaincode representation and contour following.

2.2. Enhancement using anisotropic filter

Poor binarization leads to broken ridges or touching ridges which in turn create spurious points. Our approach uses a directional anisotropic filter of elliptical shape with its major axis aligned parallel to the local ridge direction. The filter thus smoothes pixels along the ridge direction. The anisotropic filter can be expressed as (Greenberg et al., 2002; Yang et al., 1996):

$$H(x_0, x) = V + S\rho(x - x_0) \times \exp \left\{ - \left[\frac{((x - x_0) \cdot n)^2}{\sigma_1^2(x_0)} + \frac{((x - x_0) \cdot n_\perp)^2}{\sigma_2^2(x_0)} \right] \right\},$$

where n and n_\perp are mutually normal unit vectors and n is parallel to the ridge direction. The shape of the kernel is controlled by $\sigma_1^2(x_0)$ and $\sigma_2^2(x_0)$. The region constraint ρ satisfies condition $\rho(x) = 1$ when $|x| < r$ and r is the maximum support radius, which is basically determined by the size of the ellipsoid. Two additional parameters, S and V control the phase intensity (how tall the elliptical shape should be) and the peripheral pixels (near the outskirts of the kernel) respectively (Greenberg et al., 2002). We also let $V = -2$ and $S = 10$ in our experiments. $\sigma_1^2(x_0)$ and $\sigma_2^2(x_0)$ control the shape of the Gaussian kernel and must be estimated using the frequency information around x_0 . But the filter is not sensitive to their values as long as $\sigma_2^2(x_0)$ is around the measure of the average ridge width or less. In our experiments we empirically set $\sigma_1^2(x_0) = 4$ and $\sigma_2^2(x_0) = 2$. Fig. 4(a) shows the enhanced fingerprint image and Fig. 4(b) is the binary fingerprint image obtained from the enhanced image.

3. Minutiae extraction using chaincode

Most fingerprint minutia extraction methods are thinning-based where the skeletonization process converts each ridge to one pixel wide. Minutia points are detected by

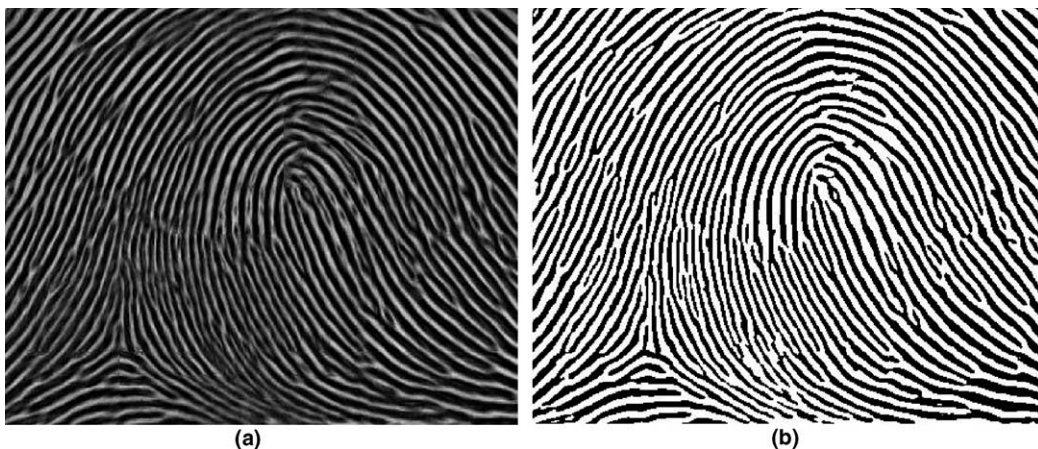


Fig. 4. Enhanced images from applying anisotropic filter based on direction field computed from chaincode: (a) Enhanced gray-scale image and (b) binary image from the enhanced image.

locating the end points and bifurcation points on the thinned ridge skeleton based on the number of neighboring pixels. The end points are selected if they have a single neighbor and the bifurcation points are selected if they have more than two neighbors (Simon-Zorita et al., 2001). However, methods based on thinning are sensitive to noise and the skeleton structure does not conform to intuitive expectation.

Our chaincode based method is obtained by scanning the image from top to bottom and right to left. The transitions from white (background) to black (foreground) are detected. The contour is then traced counterclockwise and expressed as an array of contour elements. Each contour element represents a pixel on the contour. It contains fields for the x,y coordinates of the pixel, the slope or direction of the contour into the pixel, and auxiliary information such as curvature.

In a binary fingerprint image, ridge lines are more than one pixel wide. Tracing a ridge line along its boundary in counterclockwise direction, a termination minutia (ridge ending) is detected when the trace makes a significant left turn. Similarly, a bifurcation minutia (a fork) is detected when the trace makes a significant right turn (Fig. 5(a)).

Let a vector P_{in} go in to a contour point P and a vector P_{out} go out of P . The computations of P_{in} and P_{out} use several neighboring contour points. This is to avoid local noise and at the same time obtain a better estimation of the vectors using the average of more than one point.

The significance of the direction change at P is determined by the angle made between P_{in} and P_{out} :

$$\theta = \arccos \frac{P_{in} \cdot P_{out}}{|P_{in}| |P_{out}|}$$

After size normalizations, let the two vectors be $P_{in} = (x_1, y_1)$ and $P_{out} = (x_2, y_2)$. Then,

$$\theta = \arccos(x_1 y_1 + x_2 y_2)$$

A threshold T is selected so that any significant turn satisfies the condition:

$$x_1 y_1 + x_2 y_2 < T$$

If we place the vectors in a Cartesian coordinate system with P_{in} along the x -axis (Fig. 5(b)), then the threshold T is the x -coordinate of the thresholding line. The turning direction is determined by the sign of $\sin \theta$ since the angle θ is always in the range -90° to $+90^\circ$. Thus,

$$\sin \theta = x_1 y_2 - x_2 y_1$$

Therefore $x_1 y_2 - x_2 y_1 > 0$ indicates a *left turn* and $x_1 y_2 - x_2 y_1 < 0$ indicates a *right turn*. We define the location of a minutia as the center point among the small group of turning pixels while ensuring that the minutiae density per unit area does not exceed a certain value.

4. Experimental results

We use the *Goodness Index* (GI) of the extracted minutiae to quantitatively assess the performance of our fingerprint enhancement algorithm. For both the original fingerprint images and the enhanced images, we use the adaptive binarization and then apply the chaincode minutiae extraction algorithm (Figs. 6 and 7).

We compute the *goodness* of the detected minutiae (Ratha et al., 1995; Hong et al., 1998) as

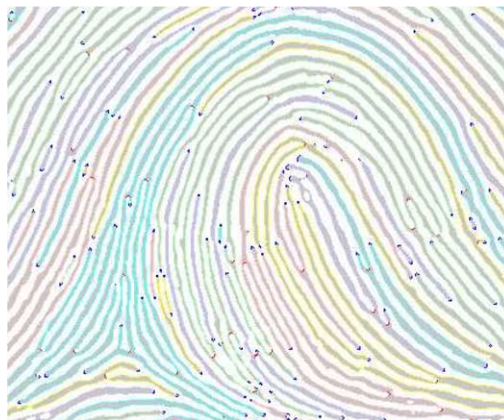


Fig. 6. Minutiae points marked in the binary fingerprint image enhanced by our method.

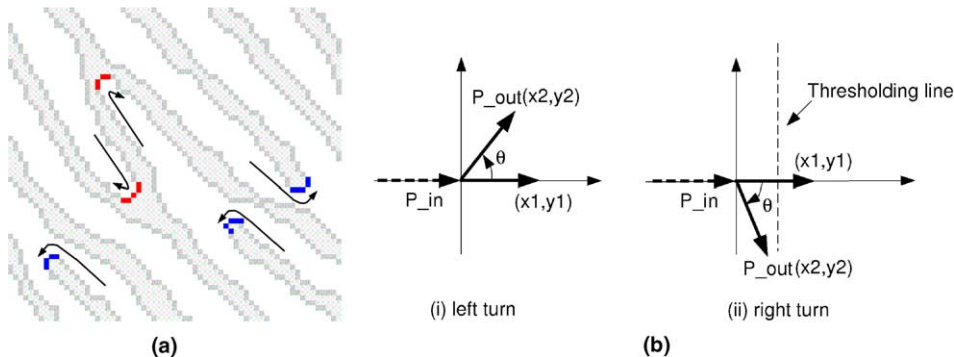


Fig. 5. (a) Minutia location in chaincode contours, the counterclockwise tracing a long the boundary of a ridge line turns left at a termination minutia and turns right at a bifurcation minutia. (b) To calculate the significant turns, the distance between the thresholding line and the y -axis gives a threshold for determining a significant turn.

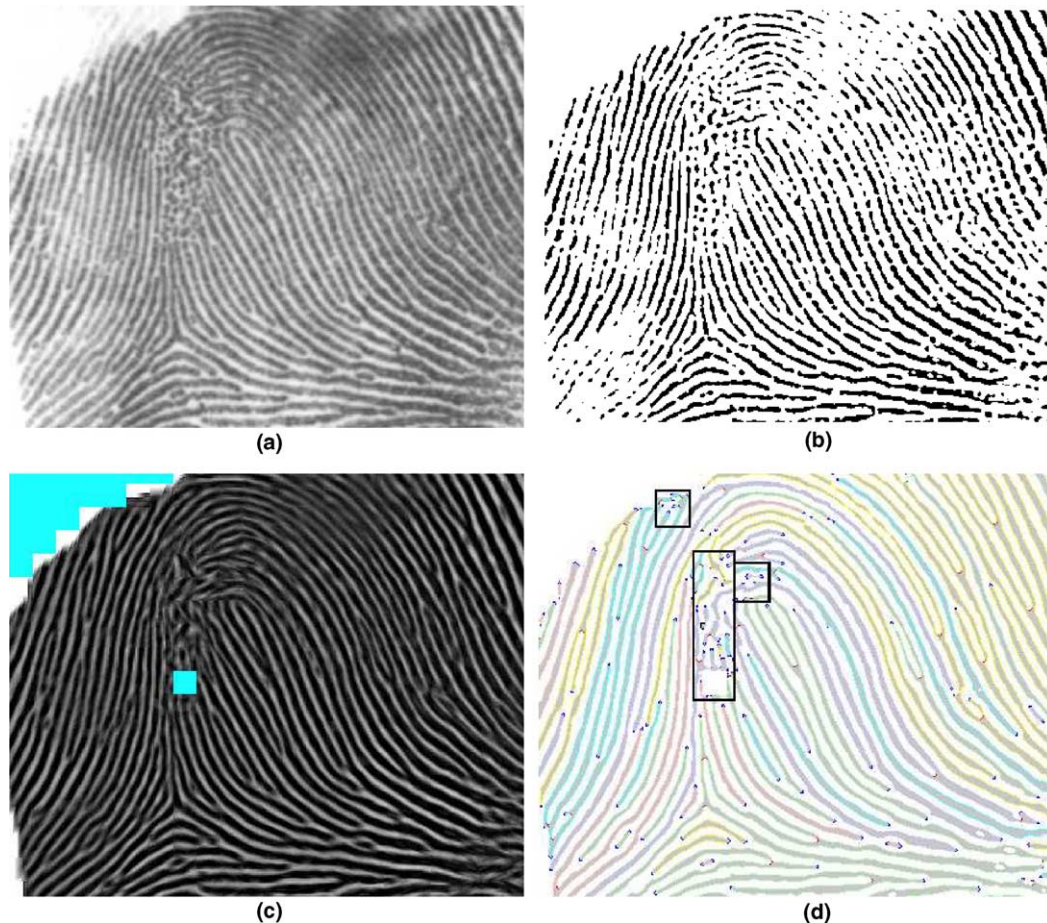


Fig. 7. Example images showing our preliminary test. (a) Original gray-scale fingerprint images, (b) its binary image from the local adaptive algorithm, (c) the image after enhancement which includes a marked box indicating an impossible area for any reliable information and (d) the candidate minutiae detected using the proposed chaincode based minutia extraction method. The marked windows show that the detected minutiae are graded automatically according to local image quality.

$$GI = \frac{\sum_{i=1}^r q_i (p_i - d_i - i_i)}{\sum_{i=1}^r q_i t_i}, \quad (1)$$

where r is the total number of 15×15 image blocks; p_i is the number of minutiae paired in the i th block; d_i is the number of missed minutiae; i_i is the number of spurious minutiae; t_i is the true number of minutiae; and q_i is a factor which represents the image quality of the i th block (good = 4, medium = 2, poor = 1). A high value of GI indicates a high reliability. The maximum value (GI = 1) is reached when all true minutiae are detected and no spurious minutiae are generated.

Our experimental set includes 20 images randomly chosen from NIST image set. In each 15×15 window, an expert determines the true minutia. An image quality index required by the GI formula is also assigned for the window. The GI indices are manually computed using the minutiae extracted from the original images. These range from 0.10 to 0.52 with an average of 0.28. After image enhancement the minutiae points are extracted again and the new GI indices range from 0.25 to 0.70 with average 0.44, which is better than the result reported in (Hong et al., 1998).

To evaluate the minutiae extraction algorithm we have chosen some sample image from FVC2004: the Third International Fingerprint Verification Competition (Maio et al., 2004) dataset. The FVC2004 dataset contains images acquired from four different sources: three fingerprint scanners and a synthetic fingerprint generation. We have taken 10 sample images from Set “B” of the database. We took 3 samples from each of DB1 and DB2 and 2 from each of DB3 and DB4. We also took another 2 images from F1 set of NIST fingerprint data set. The images are chosen to cover wide variations in image quality and results are presented in Tables 1 and 2. Table 2 also includes results of the four methods reported in (Maio and Maltoni, 1997) for comparison.

The results show that our method is comparable. Our proposed method does better in two of the three categories. The error of dropped minutiae being zero is due to the use of automatic detection of ambiguous blocks. From our experiment we found that a fingerprint includes a marked ambiguous block only if the image is very low. The false minutiae are mostly due to binarization of the difficult local area where a ridge is broken by noise or low image contrast.

Table 1
Automatic minutiae detection

| Fingerprint | Minutiae | d | f | x |
|--------------|----------|-----|-----|-----|
| DB1_B_101_2 | 38 | 0 | 7 | 2 |
| DB1_B_103_1 | 36 | 0 | 8 | 0 |
| DB1_B_104_4 | 29 | 0 | 10 | 2 |
| DB2_B_101_1 | 30 | 0 | 17 | 1 |
| DB2_B_106_3 | 33 | 0 | 10 | 3 |
| DB2_B_110_1 | 26 | 0 | 27 | 2 |
| DB3_B_101_3 | 32 | 0 | 10 | 1 |
| DB3_B_105_2 | 37 | 0 | 14 | 1 |
| DB4_B_103_5 | 48 | 0 | 20 | 4 |
| DB4_B_110_3 | 34 | 0 | 41 | 3 |
| NIST_f000001 | 113 | 0 | 28 | 3 |
| NIST_f000089 | 82 | 0 | 16 | 7 |

The numbers of minutiae are manually detected. d , f and x denote the number of dropped minutiae, false minutiae and exchanged minutiae, respectively.

Table 2
Average errors

| | A (%) | E (%) | B (%) | C (%) | Our method (%) |
|--------------------|-------|-------|--------|--------|----------------|
| Dropped minutiae | 4.51 | 1.75 | 1.50 | 5.01 | 0 |
| False minutiae | 8.52 | 22.56 | 111.28 | 203.01 | 38.67 |
| Exchanged minutiae | 13.03 | 9.52 | 7.02 | 8.77 | 5.39 |
| Total error | 26.07 | 33.83 | 119.80 | 216.79 | 44.06 |

The average results of the proposed method comparing with the results of the four methods (A, B, C and E) reported in (Maio and Maltoni, 1997).

5. Conclusions

This paper describes novel use of chaincode image representation in fingerprint image enhancement and minutiae extraction. The chaincode representation allows efficient image quality enhancement and detection of fine minutiae feature points. For image enhancement a given fingerprint image is first binarized after a quick averaging to generate its chaincode representation. The direction field is estimated from a set of selected chaincodes. The original gray-scale image is then enhanced by a filtering algorithm. For feature extraction, the enhanced fingerprint image is binarized using a locally adaptive binarization algorithm for generating the chaincode representation. The minutiae are detected using a sophisticated ridge contour following procedure. Subjective experiment shows that the method is very effective.

Since chaincode representation is for binary images, the quality of the binary images are important. Although at the enhancement stage we only need a binary image good enough for the chaincode-based method to be able to compute a reliable direction field, we still feel the need of a better preprocessing for the binarization.

For feature extraction, the chaincode method is an efficient method using binary images. Our future work is directed on a post-processing method for removing added minutiae and exchanged minutiae due to attached noise from sweat pores and dots in between ridges.

Acknowledgements

We would like to thank Chaohong Wu and Tsai-yang Jea for their assistance in implementing some of the techniques described in this paper.

References

- Donahue, M.J., Rokhlin, S.I., 1993. On the use of level curves in image analysis. *Image Understanding* 57 (2), 185–203.
- Feldbach, M., Tonnies, K.D., 2001. Line Detection and Segmentation in Historical Church Registers. In: Sixth Internat. Conf. on Document Analysis and Recognition, Seattle, USA, September 2001. IEEE Computer Society, pp. 743–747.
- Giuliano, E., Paitra, O., Stringa, L., 1977. Electronic Character Reading System, US Patent No. 4047152, September 6.
- Greenberg, S., Aladjem, M., Kogan, D., 2002. Fingerprint image enhancement using filtering techniques. *Real-Time Imaging* 8, 227–236.
- Hong, L., Wan, Y., Jain, A., 1998. Fingerprint image enhancement: algorithm and performance evaluation. *IEEE Trans. Pattern Anal. Machine Intell.* 20, 777–789.
- Jain, A.K., Hong, L., Pankanti, S., Bolle, R., 1997. An identity authentication system using fingerprints. *Proc. IEEE* 85 (9), 1365–1388.
- Jain, A., Hong, L., Bolle, R., 1997. On-line fingerprint verification. *IEEE-PAMI* 19 (4), 302–314.
- Lee, H.C., Gaensslen, R.E., 1991. *Advanced Fingerprint Technology*. Elsevier, New York, NY.
- Madhvanath, S., Kim, G., Govindaraju, V., 1997. Chain code processing for handwritten word recognition. *IEEE Trans. Pattern Anal. Machine Intell.* 21, 928–932.
- Maio, D., Maltoni, D., 1997. Direct gray-scale minutiae detection in fingerprints. *IEEE Trans. Pattern Anal. Machine Intell.* 19, 27–40.
- Maio, D., Maltoni, D., Cappelli, R., Wayman, J.L., Jain, A.K., 2004. FVC2004: Third Fingerprint Verification Competition. In: Proc. Internat. Conf. on Biometric Authentication (ICBA), Hong Kong, July 2004, pp. 1–7.
- Moenssens, A., 1971. *Fingerprint Technology*. Chilton Book Company, London.
- O’Gorman, L., Nickerson, J.V., 1989. An approach to fingerprint filter design. *Pattern Recognition* 22, 29–38.
- Ratha, N.K., Chen, S., Jain, A., 1995. Adaptive flow orientation-based feature extraction in fingerprint images. *Pattern Recognit.* 28 (11), 1657–1672.
- Ratha, N., Karu, K., Chen, S., Jain, A., 1996. A real time matching system for large fingerprint databases. *IEEE-PAMI* 18 (8), 799–813.
- Schneider, J.K., Glenn, W.E., 1996. Surface Feature Mapping Using High Resolution C-Span Ultrasonography. US Patent 5587533.
- Sherlock, D., Monroe, D.M., Millard, K., 1994. Fingerprint enhancement by directional Fourier filtering. In: *IEEE Proc. on Visual Imaging Signal Processing*, vol. 141, pp. 87–94.
- Shi, Z., Govindaraju, V., 1997. Segmentation and recognition of connected handwritten numeral strings. *J. Pattern Recognition* 30 (9), 1501–1504.
- Simon-Zorita, D., Ortega-Garcia, J., Cruz-Llanas, S., Sanchez-Bote, J.L., Glez-Rodriguez, J., 2001. An improved image enhancement scheme for fingerprint minutiae extraction in biometric identification. In: Bigun, J., Smeraldi, F. (Eds.), Proc. Third Internat. Conf. on Audio- and Video-Based Biometric Person Authentication AVBPA’01, Halmstad, Sweden, June 2001, LNCS2091, pp. 217–222.
- Wilf, A.M., 1981. Chaincode. *Robotics Age* 3 (2).
- Xia, X., O’Gorman, L., 2002. Innovations in fingerprint capture devices. *J. Pattern Recognition* 36 (2), 361–370.
- Yang, G.Z., Burger, P., Firmin, D.N., Underwood, S.R., 1996. Structure adaptive anisotropic filtering. *Image Vision Comput.* 14, 135–145.